A Novel Impedimetric Sensor Based on Cyanobacterial Extracellular Polymeric Substances for Microplastics Detection

Wejdene Gongi[1,2] · Hassen Touzi[3] · Idris Sadly[2] · Hafedh Ben ouada[3] · Ollivier Tamarin[2,4] · Hatem Ben ouada[1]

Accepted: 10 August 2022 / Published online: 21 August

Abstract
Cyanobacterial extracellular polymeric substances "EPS" have attracted intensive concern in biomedicine and food. Nevertheless, the use of those polymers as a sensor coating material has not yet been investigated mainly for microplastic detection. This study focuses on the application of EPS as a sensitive membrane deposited on a gold electrode and investigated with electrochemical impedance spectroscopy to detect four types of microplastics with a size range of 0.1 µm to 1 mm. The surface properties of this impedimetric sensor were investigated by Scanning electron microscopy, Fourier transforms infrared spectroscopy, and X-ray spectroscopy and, showed a high homogenous structure with the presence of several functional groups. The EPS-based sensor could detect the four tested microplastics with a low limit of detection of 10^{-11} M. It is the first report focusing on EPS extracted from cyanobacteria that could be a new quantification method for low concentrations of microplastics.

Keywords Extracellular polymeric substances · Impedimetric biosensor · Electrochemical impedance spectroscopy · Microplastics detection

Introduction

Over the past century, the production and demand for plastic have grown exponentially, especially during the global coronavirus outbreak. Plastic waste has thus become a worrying source of contamination [1]. Plastics stay in ecosystems for centuries because they are not biodegradable [2]. They turn into small particles with a diameter between 5 nm and 100 mm, defined as microplastics. Microplastics were quantified in freshwater environments, including lakes, rivers, surface waters, reservoirs, and river sediments [3–5].

These particles present severe and widespread ecological impacts [5]. They are transmitted through the trophic chain, altering the expression of genes in many aquatic organisms, causing toxic effects and endocrine disruption and adverse effects on the reproductive, neurological and immunological systems in humans and animals [6, 7]. Thus, it is crucial to identify plastic particles and determine their size and concentration both in the laboratory and in the natural environment.

Conventional measurement techniques for identifying and measuring microplastics (MP) in the field or the laboratory have been the subject of several reviews [8–11]. They can be summarized into three types of methods (Supplementary Table 3). (i) Visual methods using the naked eye or stereomicroscope or scanning electron microscopy (SEM) have often been applied for the identification of plastic in general [12]. They can be combined with staining using Nile red [13] or with energy dispersive spectroscopy using X-rays to identify elemental composition in addition to particle size [14]. (ii) More sophisticated methods used included microplastic degradation by pyrolysis [15] or thermal degradation, followed by gas chromatography–mass spectrometry analysis [16]. These techniques often overlap with visual methods for the identification and quantification of microplastic types

✉ Wejdene Gongi
gongi.wejden@gmail.com

1 Laboratory of Blue Biotechnology & Aquatic Bioproducts, National Institute of Marine Sciences and Technologies, 5000 Monastir, Tunisia

2 University of French Guiana, Espace-Dev, UMR 228, 97300 Cayenne, France

3 Laboratoire des Interfaces et Matériaux Avancés, Faculté des Sciences de Monastir, Monastir University, 5000 Monastir, Tunisia

4 Université de Bordeaux, CNRS, Bordeaux INP, IMS, UMR 5218, 33400 Talence, France

[10]. (iii) The most used methods that showed promising results [17, 18] are based on the spectral signature of plastic polymers. They included Fourier-transform infrared (FTIR) methods as attenuated total reflection-FTIR (ATR-FTIR) [19, 20] or FTIR imaging [19, 21], and Raman spectroscopy analysis as Raman microspectroscopy [22, 23] or Raman imaging [24].

Overall, conventional methods for the identification and/or quantification of microplastics are subject to several limitations in terms of accuracy, time and cost of analysis [10, 11]. Samples often require heavy pre-treatment in the laboratory to avoid artefacts generated by organic or inorganic particles other than microplastics [25, 26]. Additionally, microplastics are usually highly dispersed in water bodies, requiring additional concentration processes to reach the detection limit of the analytical device. This preprocessing is time-consuming and labor-intensive.

Simpler and cheaper analytical methods are needed and, in this sense, biosensors have received great attention [27–29]. Biosensors belong to a category of analytical devices capable of providing a measurable output signal using the recognition of a substance of interest via a biological recognition unit. The main advantages of biosensors are low cost, low detection limit and fast sensitivity, allowing real-time and in situ monitoring [30]. So far, the detection of microplastics by biosensors and by sensors is at the stage of investigation despite the potential offered by these systems. In [31], the authors combined two optical methods (interference and specular reflection of light) to design a prototype optical sensor to detect translucent microplastics in fresh water. Malyuskin [32] used a microwave resonance spectroscopy sensor to detect and quantify microplastics in soil and water at parts per thousand concentration levels.

Several biosensors based on enzymes, antibodies, nucleic acids and algal cells have been used as biorecognition elements [33–36]. They have demonstrated their effectiveness in the detection of different pollutants, including heavy metals, pharmaceutical pollutants, pesticides and biological contaminants. Recently, the efficiency of peptide biosensors for the detection of polystyrene and polypropylene microparticles in their unoxidized and oxidized forms was demonstrated [37]. Enzyme-based biosensors have also been shown to be effective in detecting nano and microplastics [38]. Huang et al. [39] detected low levels of microplastics by developing a surface plasmon resonance biosensor, using immobilized estrogens as bioreceptors. However, further progress is needed for a better and more acceptable detection process. In particular, the search for bioreceptors with a strong affinity for different types of microplastics while inducing a reliable and reproducible signal remains relevant.

Cyanobacterial extracellular polymeric substances (EPS) have attracted great attention and have been extensively studied for several applications due to their unique and diverse properties [40]. EPS are relatively easy to obtain, do not pose any ethical problems and could be used in bioremediation and bioleaching due to their great structural, physical and chemical diversity [41]. They are also potential candidates for the production of biofilms and thus replace the use of hazardous plastic materials [42]. Additionally, EPS have been used as a metal-binding material due to the abundance of negatively charged amino acids like aspartic acid and glutamic acid in their structure [43, 44]. These complex molecules can establish London forces, electrostatic interactions, hetero-aggregates and hydrogen bonds in the adhesion and cohesion of microplastic particles [45, 46].

These properties represent advantages for the use of cyanobacterial EPS as bioreceptors in the development of biosensors intended for the detection of microplastics.

In this context, this article presents a first investigation aimed at the development of an EPS-based biosensor for the detection of microplastics. It focuses on the microplastics most frequently found in marine wastewater effluent, including PS (polystyrene), PA (polyamide), PMA (polymethyl acrylate) in the form of nylon, and PE (polyethylene low density) in the form of polyester. Electrochemical impedance spectroscopy (EIS) was used to analyze the interaction between microplastics and EPS. EIS has been frequently used to characterize the stepwise modification of several biosensors [33, 47].

The main objectives of the current study are: (1) elaborate and characterize an EPS film solution; (2) immobilize and validate the EPS adhesion to a gold wafer electrode; (3) characterize the surface sensor using several techniques. Namely, Fourier transforms infrared spectroscopy (FTIR), Scanning electron microscopy (SEM), and X-ray spectroscopy (XRD) characterize the elaborated device by EIS measurements; and finally (5) investigate its analytical performances.

Materials and Methods

Extraction, Elaboration and Characterization of the EPS Film Forming Solution

Extracellular Polymeric Substances (EPS) were extracted from the culture cultivation of the cyanobacteria *Gloecapsa gelationosa*. The EPS was concentrated using a tangential ultra-filtration cell (Vivaflow 50) in Millipore membranes with 5 kDa pore size and then washed with deionized water until constant conductivity to eliminate low molecular weight substances [48, 49]. Lastly, the recovery filtrate was freeze-dried, lyophilized, and weighed for EPS content determination. The film-forming solution was prepared by dissolving 1 mg of *Gloecapsa* EPS in 1 mL ethanol solution (99% of purity, purchased from Sigma Aldrich). In order to ensure the complete

dissolution of the EPS in the ethanolic solution, the pH was regulated at a value of 12.

The biochemical composition of the EPS film-forming solution was characterized using colorimetric and gravimetric methods. Total carbohydrates content was determined by the phenol sulphuric acid method [50] using d-glucose (Sigma, 50-99-7) as standard. Proteins content was determined according to Lowry et al. [51] using bovine serum albumin (Sigma, 10711454001) as standard. The sulphate groups were calorimetrically calculated using potassium sulphate as standard [52].

The zeta potential of the EPS film forming solution was measured on Zeta size 3000 HS. (Malvern, UK). Each sample was repeatedly measured 3 times and the values reported are the mean value ± standard deviation for two replicate samples. The measurements were performed in triplicate at 25 ± 1 °C by measuring the electrophoretic mobility of the dispersed particles in a charged field. The software to convert the electrophoretic mobility measurements into zeta potential values used the Smoluchowsky mathematical model [53].

Sensor's Elaboration

The sensor was elaborated according to the method described by Touzi et al. [54]. In this study, we evaluated the applicability of the EPS as a sensitive membrane of gold wafers transducer. The gold wafers were cleaned with acetone and treated with heated piranha solution (H2O2/H2SO4 mixture 3:7 v/v) before being rinsed in ultrapure water and then dried under nitrogen flow.

The immobilization of sensitive EPS film on the cleaned gold surface was performed by means of spin-coating. A drop (10 µL) of EPS film solution was deposited on a rotating gold wafer at a speed of 2000 rpm for 20 s. The resulting thin film on gold wafers was stabilized before use by drying (60 °C for 1 h) and soaking overnight in a 0.01 M acetate buffer solution.

Surface Characterization of the Sensitive Membrane

The surface of the EPS sensitive membrane was observed by Scanning electron microscopy (SEM), Fourier transform infrared spectroscopy (FTIR), and X-ray spectroscopy (XRD).

SEM analyses were performed using an HR-FESEM SU-70 Hitachi microscope, operating at 4 kV in the field emission mode and an angle of 90° with the surface, using different magnifications. Before imaging, samples were cryo-fractured by immersion in liquid nitrogen and fixed on the SEM support using double-sided adhesive tape, and observed under an accelerating voltage of 5.0 kV and absolute pressure of 60 Pa, after sputter coating with a 5 nm thick gold.

FTIR analyses were performed using a Perkin–Elmer system (Perkin-Elmer) equipped with an attenuated total reflectance (ATR) cell. The spectra were recorded at room temperature, in the range of 500–4000 cm^{-1} with a resolution of 2 cm^{-1} and, evaluated by Agilent software.

Diffraction data of the EPS gold sensor membrane was collected with an X-ray diffractometer CICECO Empyrean (JDX 3532; Japan) equipped with CuKα radiation (λ = 1.54184A), a 4-circle kappa goniometer, and a CCD Detector. Data collection and processing were carried out using CrysAl-isPro Software System. The diffraction angle range of observation was 5° to 50°.

Electrochemical Impedance Spectroscopy « EIS »

Impedance spectroscopy measurements were carried out at room temperature (20 ± 3 °C) in an electrochemical cell (Pyrex glass of 5 mL volume) connected to an impedance analyzer and controlled by a computer. Three electrodes electrochemical cells were used: the modified gold electrode as the working electrode (0.19 cm^2 active area defined by an *O*-ring seal), a platinum counter-electrode and a saturated calomel electrode (Ag/AgCl/KCl) used as a reference electrode (Fig. 1). Ammonium acetate (CH_3CO_2–NH_4^+) aqueous solution (4 mL, 0.01 M at pH 6.8) was used as a background electrolyte. The excitation sinusoidal signal was 10 mV of amplitude to provide a linear response of the cell, which means a sinusoidal current response at the same frequency and shifted in phase. The frequency was scanned in a range of [10^{-3} Hz, 10^6 Hz]. Many Factors induce destabilization of the response of the cell. A delay time is always needed to achieve a steady state. This stabilization was detected by the reproducibility of the response. In our case, a delay of 90 min was sufficient to minimize the drift in the system. The response of the EIS was investigated by Nyquist diagrams according to the microplastics. All our measurements were done at the negative bias of − 0.3 V which allows a great definition of the Nyquist plot and is not too high to induce the corrosion phenomenon. The equivalent circuit parameters for the electrolyte interface of the functionalized surface of EPS were directly deduced from the experimental data by applying the software Nova Autolab 1.5, after testing several models of the equivalent circuit.

Microplastics Solution

Four types of spherical-shaped microplastics, used in this study, including polystyrene (PSS) in size 0.1 µm, polymethylacrylate (PMA) in size 10 µm; Nylon polyamide (PA) in size 50 µm and low-density polyethylene (PE) in size 1 mm were purchased from Sigma-Aldrich as aqueous suspensions

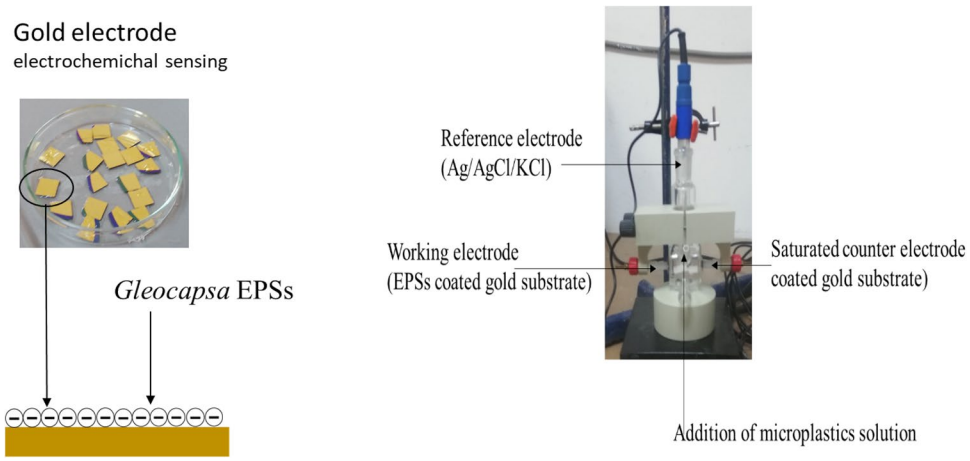

Fig.1 Scheme for the Gleocapsa EPS immobilization on the electrochemical sensor gold wafer (left) and the three electrochemical electrodes (right)

at 10% solid concentration. The microplastic solutions were prepared in water solution at different concentrations from 10^{-11} to 10^{-5} M.

Results and Discussion

Characterization of the EPS Film-Forming Solution

The chemical composition, particle size, and zeta-potential values of the film-forming solution are reported in Table 1. The chemical composition revealed that EPS solutions are principally composed of carbohydrates fraction. The total carbohydrate content was 70% of dry weight. The protein content was evaluated at 12%. The relatively high ratio of ester-sulfated groups (10%) proposes that the solution is of sulfated hetero-polysaccharides nature. The present results are in agreement with that found in the literature that revealed that several cyanobacterial EPS substances are sulfated polysaccharides [41, 55].

In general, polymers of polysaccharide nature are known for their ability to physical trapping or inclusion of several particles' material [56]. Furthermore, the presence of peptides confers on EPS the possibility of adsorbing MPs by hydrophobic binding [37].

From the results of the zeta potential listed in Table 1, it was found that the EPS film-forming solution had negative charges of − 41 mV. The negative-charged cyanobacterial exopolysaccharides are commonly reported by other authors and attributed to the presence of anionic groups and uronic acids [44, 57]. However, according to our investigations, the Zeta potential varied with the pH of the EPS film forming solution. At pHs below 10, the value of the Zeta potential was + 30 mV (data not shown), but under these conditions the dissolution of the EPS is only partial. It is for this reason that we have maintained the pH of the EPS solution at 12 throughout the work, which guarantees the stability of the ionic charge and the homogeneity of the solution.

The typical average particle size distribution of the EPS film solution is plotted in Fig. 2. Particle size distributions showed monomodal shape dominated by small particles size of around 100 nm. The homogeneity of particle size distribution is confirmed by the low polydispersity index 0.036 (Table 1). According to Danaei et al. [58] a PDI lower than 0.05 indicate a highly monodisperse character. Small particle size polymers with low PDI have a great capacity to bind uniform micro-nanoparticles by encapsulation, electrostatic interaction or by covalent conjugation [58].

Characterization of the Sensor Surface

The surface of the EPS sensor membrane was observed by Scanning electron microscopy (SEM), Fourier transforms infrared spectroscopy (FTIR) and, X-ray spectroscopy (XRD).

The SEM top view and cross-section (Fig. 3) of the EPS membrane confirmed the homogeneous character and revealed a microstructural lamellar feature.

The presence of functionalities on the surface of the sensor was identified by FTIR measurements as shown in Fig. 4, revealing prominent functional reactive groups, such as sulfate, hydroxyl, or carboxylic. A broad band in

Table 1 Chemical composition: carbohydrates, protein, sulfate, mean particle size, and zeta potential of EPS film-forming solution

Proteins	Sulfate	Carbohydrates	Mean diameter (nm)	Polydispersity index	pH	Zeta potential (mV)
12.2 ± 0.02	10.1 ± 0.1	70.2 ± 0.1	99.7 ± 2.0	0.036 ± 0.001	12	− 41.2 ± 3.5

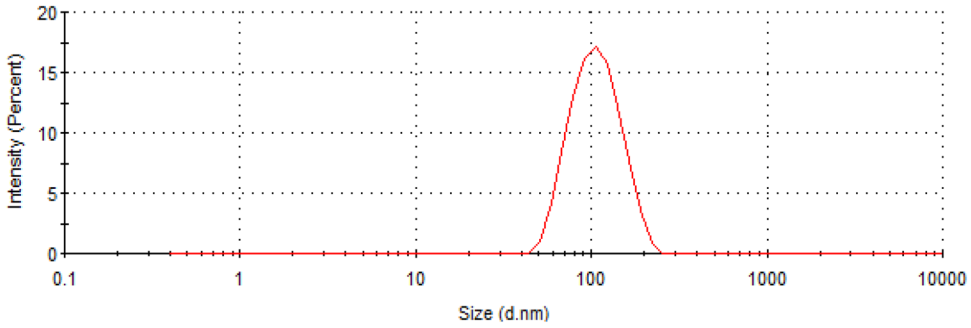

Fig. 2 Size distribution of the EPSs film-forming solution

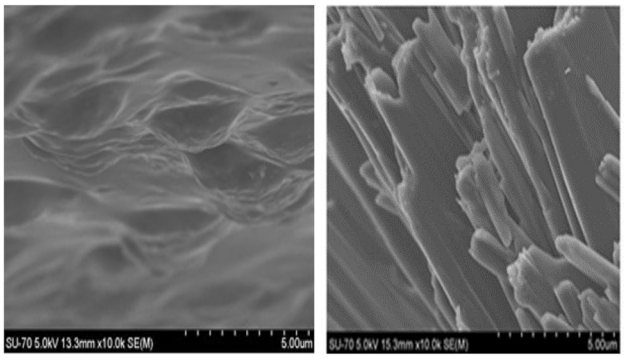

Fig. 3 Top-view SEM images of the EPS sensor membrane

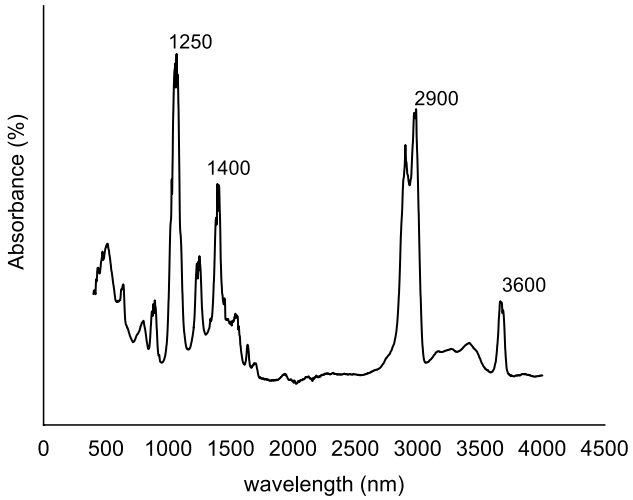

Fig. 4 Infrared spectra of the Gloecapsa gelatinosa EPS sensor membrane

the range of 2900–3600 cm^{-1} is attributed mainly to the stretching vibration (ν) of νO–H or νC–H groups, typical of the hydroxyl and alkyl functionality of carbohydrates [59]. The prominent absorption observed at the region 1400 cm^{-1}

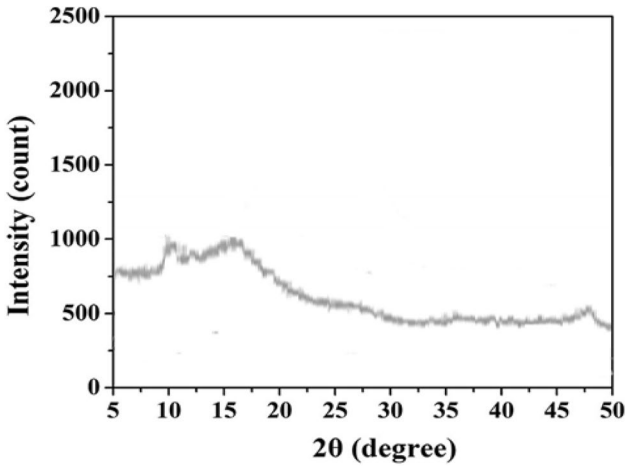

Fig. 5 Representative XRD profile of the Gloecapsa gelatinosa EPS sensor membrane

could be attributed to the bending vibration (δ) of δN–H and the νC–N [60] indicating the existence of amino acids from peptide/proteins. The important peak observed at 1250 cm^{-1} corresponds to the stretching vibration of the ester sulfate groups (S=O) [60] and is further evidence of the hetero-sulfated polysaccharides nature [61, 62].

In this regard, the plastic binding capacity would be directly proportional to the availability of these functional groups at the surface [63]. Restrepo-Flórez et al. [64] reported that the interaction between polymers/organisms and plastic particles leads to changes in functional groups and physical properties of plastic. However, as far we know, no studies have analyzed these interactions in depth.

X-ray spectroscopy (XRD) is a rapid analytical technique most widely used for phase identification of crystalline material. The XRD profile of the EPS membrane surface (Fig. 5) did not exhibit well-differentiated peaks, suggesting an amorphous nature. Similar to previous profiles of native EPSs produced by several microorganisms [52, 65].

Impedance Measurements and Equivalent Circuit Modeling

The electrochemical measurement is well-suited to detect changes in the electrode-medium interface [66]. Thus, in the field of biosensors, monitoring the immobilization procedure of the recognition element is based on the measurement of the electrochemical impedance variation. EIS is a steady-state technique using low amplitudes signal analysis and detect signal relaxations over a very wide range of applied frequency. The Impedance measurement results are illustrated in the Nyquist plot using the imaginary part (Z″) and the real part (Z′) of impedance (Z). To design the electrical model of the electrochemical cell, we consider the gold-EPS interface in series with the EPS membrane and in series with the electrolyte solution. The model of the electrolyte solution should be a resistor Rs, the interface gold- EPS is modeled by a real capacitor (i.e. a capacitance CdL in parallel with a resistor Rct) and the membrane EPS is assumed to another real capacitor with a capacitance Cm and a resistance Rm. The three dipoles are assembled in series. CdL is the double layer capacitance and Rct is the charge transfer resistor. This model is denoted R(C//R)(C//R). In the Nyquist plot, the dipole C//R correspond to a semi-circle with a diameter R. In the case of a semi-circle whose center is shifted towards the negative Z″, we replace the capacitance C with a constant phase element CPE. The constant phase element is considered as a "power-law-dependent specific layer capacitance". The constant phase element reflects non-homogeneity and defecting area of the electrode surface. (Rct) corresponds to the electron transfer resistance between the bulk and the electrode's surface [67]. In our specific case, to take into account our EPS chemical layer immobilized on the electrode surface, the model "R(CPE//R)(CPE//R)" become "Rs (CPE_EPS//Rm)(CPE_dL//Rct)".

In this work, the equivalent electrical circuit models Rs(CPE_EPS//Rm) (*i.e.* without the modelization of the interface between the gold substrate and the EPS film), and Rs(CPE_EPS//Rm)(CPE_dL//Rct) have been tested. Based on the chi-square values of each model fitting, the Nyquist diagrams obtained for the gold electrode after the EPS deposition (Fig. 6) show that Rs(CPE_EPS//Rm)(CPE_dL//Rct)

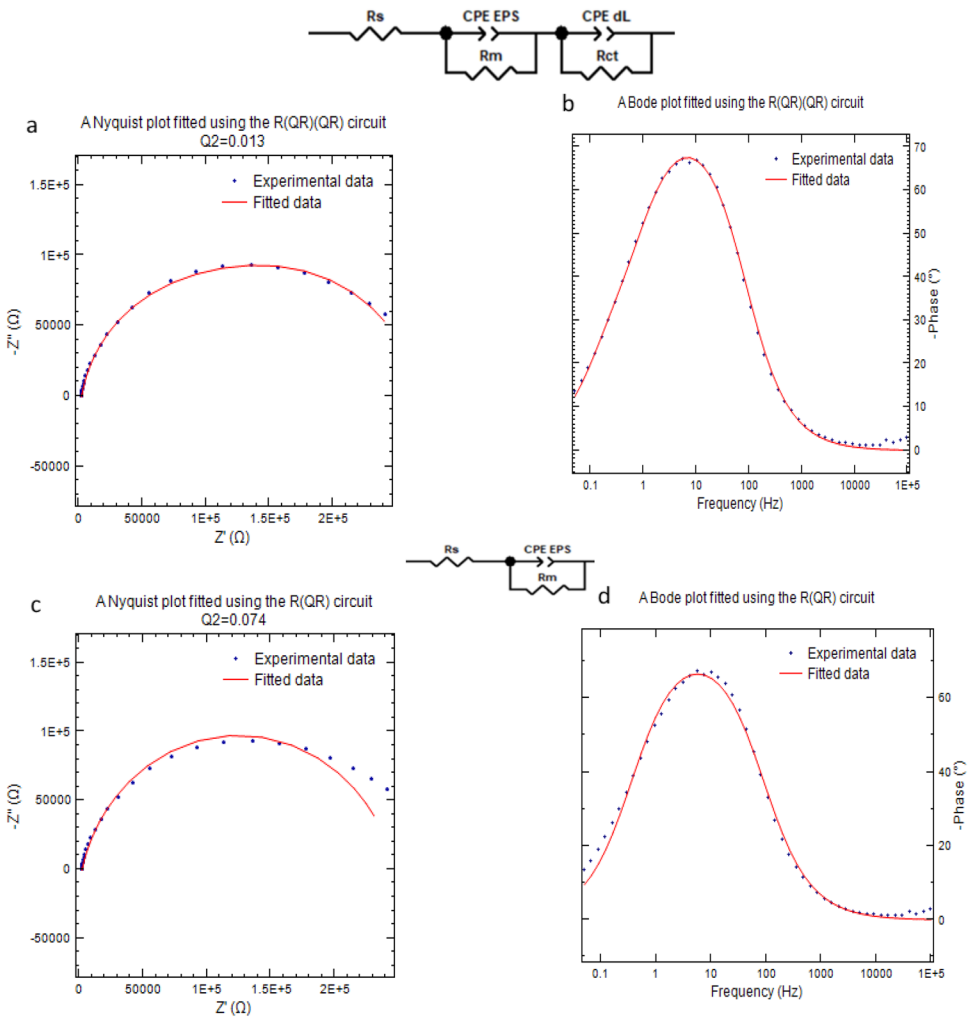

Fig. 6 **a** A Nyquist plot fitted using the Rs(CPE_EPS//Rm)(CPE_dL//Rct) circuit. **b** A Bode plot fitted using the Rs(CPE_EPS//Rm)(CPE_dL//Rct) circuit. **c** A Nyquist plot was fitted using the Rs(CPE_EPS//Rm) circuit. **d** A Bode plot fitted using the Rs (CPE_EPS//Rm) circuit. Z″: imaginary part of impedance and (Z′) the real part of impedance Rs: solution resistance; Rm: resistance of the EPS film; CPE_EPS: constant phase element of the EPS film; CPE_dL: constant phase element of the interface; Rct: charge transfer equivalent resistance; χ^2: chi-square.

circuit was more suitable (corresponding chi-square values $\chi^2 = 0.013$) for describing the EPSs gold sensor for microplastics detections. The observed non symmetric profile (Fig. 6 b) of the phase spectra confirms this choice. The good agreement between the measured data and the fitting curves indicates that this equivalent circuit is suitable and meaningful for this electrochemical system and is therefore used to fit the impedance spectroscopy data and extract Rs, Rm, CPE_EPS, Rct, and CPE_dL values. These were obtained by plot fitting with a less than 5.0% error percentage (Table 2).

Influence of Microplastics on the Electrochemical Response

Nyquist diagrams resulting from electrochemical impedance spectroscopy were plotted (Fig. 7) at different concentrations ranging from 10^{-11} to 10^{-5} M of each studied microplastics (PSS, PMA, PA, and PE).

The system stability for application as a sensor was recorded after the EPSs film deposition. The Nyquist diagram corresponding to the blank representing EPS without microplastics (EPS acetate) showed a semicircle with a Z′ value of 1 E^{+5} to 1.5 E^{+5} Ω suggesting a high stability of the EPS electrode. The shape of Nyquist plots is dependent mainly on the electrochemical responses taking place at the surface of the working EPS electrode. A difference in the electrical signal was created due to the kinetic binding of each type of microplastics at the sensors surface. The electrochemical sensor was able to detect all tested microplastics at a very low concentration of 10^{-11} M.

The differences monitored between the four experimented types of plastics was mainly related to their sizes. By comparing the Nyquist diagrams, a fast saturation of the sensor membrane was detected in the case of PA at a concentration of 10^{-10} M and of PE at a concentration of 10^{-11} M. The real impedance Z′ was evaluated in these cases respectively at 1.8 E^{+5} and 2.5 $E^{+5}\Omega$. This behavior could be mainly correlated to the high size of both PA (50 µm size) and PE (1 mm size) that blocks EPSs micropores. It was reported that the plastics size affects the ability of polymers to adsorb particles [68, 69].

On other hand, the diameter of the semicircle increased with increasing the concentration of both PMA (10 µm) and PSS (0.1 µm). A detection limit was observed at 10^{-6} M in the case of PMA and 10^{-5} M in the case of PSS. At all tested concentrations, PSS showed the highest Z′ value, higher than that recorded with PMA, thereby indicating more affinity of EPS sensor to detect large range of PSS than the other types of microplastics.

Table 2 shows the different results obtained after fitting the experimental data, revealing that the detection was influenced by the microplastic concentrations. Little variation was observed in constant phases elements of both the

Table 2 Parameters of the electrical circuit equivalent to the EPS electrode for different concentrations (10^{-11} to 10^{-5} M) of microplastics: PA, PMA, PSS, and PE (values are reported until saturation)

	Rs (kΩ)	Rm (KΩ)	CPE EPS (µF)	µ	Rct (KΩ)	CPE dL (µF)	µ
EPS-acetate	3.4 ± 0.5	127.6 ± 2.0	2.8 ± 0.0	0.9 ± 0.0	59.4 ± 1.3	1.8 ± 0.2	0.9 ± 0.0
PA $10E^{-11}$	3.0 ± 0.3	121.0 ± 2.2	3.2 ± 0.5	0.9 ± 0.0	60.8 ± 1.2	1.8 ± 0.0	0.9 ± 0.0
PA ($10E^{-10}$–$10E^{-5}$)	2.1 ± 0.2	177.1 ± 1.9	3.3 ± 0.5	0.8 ± 0.0	60.8 ± 1.2	1.7 ± 1.0	0.9 ± 0.0
PSS $10E^{-11}$	3.3 ± 0.1	118.5 ± 4.3	3.0 ± 0.6	0.9 ± 0.0	60.3 ± 2.2	1.8 ± 0.7	0.9 ± 0.0
PSS $10E^{-10}$	2.5 ± 0.5	142.0 ± 3.2	3.2 ± 0.8	0.9 ± 0.0	60.0 ± 2.3	1.7 ± 0.9	0.9 ± 0.0
PSS $10E^{-9}$	1.9 ± 0.2	168.2 ± 2.2	3.3 ± 0.2	0.9 ± 0.0	59.3 ± 2.0	1.8 ± 0.0	0.9 ± 0.0
PSS $10E^{-8}$	1.8 ± 0.6	195.0 ± 2.0	3.5 ± 0.3	0.9 ± 0.0	58.3 ± 2.1	1.5 ± 0.1	0.9 ± 0.0
PSS $10E^{-7}$	1. 7 ± 0.5	223.1 ± 2.2	3.7 ± 0.8	0.9 ± 0.1	54.8 ± 1.2	1.5 ± 0.2	0.9 ± 0.0
PSS $10E^{-6}$	1.6 ± 0.2	252.4 ± 2.0	3.9 ± 0.7	0.9 ± 0.1	52.4 ± 2.2	1.4 ± 0.3	0.9 ± 0.0
PSS $10E^{-5}$	1.41 ± 0.54	267.76 ± 2.4	3. 9 ± 0.5	0.9 ± 0.1	49.1 ± 1.8	1.4 ± 0.5	0.9 ± 0.1
PE ($10E^{-11}$–$10E^{-5}$)	2.4 ± 0.7	208.3 ± 2.5	4.0 ± 0.4	0.9 ± 0.0	59.4 ± 2.2	1.1 ± 0.2	0.9 ± 0.1
PMA $10E^{-11}$	3.5 ± 0.9	171.9 ± 3.2	2.2 ± 0.3	0.9 ± 0.0	65.9 ± 2.0	1.7 ± 0.1	0.9 ± 0.0
PMA $10E^{-10}$	3.2 ± 0.2	189.1 ± 3.5	2.7 ± 0.2	0.9 ± 0.0	64.9 ± 1.7	1.7 ± 0.0	0.9 ± 0.0
PMA $10E^{-9}$	3.1 ± 0.9	245.3 ± 4.0	2.8 ± 0.6	0.9 ± 0.0	51.7 ± 2.2	1.6 ± 0.1	0.9 ± 0.0
PMA $10E^{-8}$	2.0 ± 0.9	274.8 ± 4.6	2.8 ± 0.8	0.9 ± 0.1	54.8 ± 1.3	1.5 ± 0.3	0.9 ± 0.0
PMA $10E^{-7}$	2.0 ± 0.5	292.3 ± 2.0	3.2 ± 0.3	0.9 ± 0.0	51.6 ± 3.2	1.5 ± 0.1	0.9 ± 0.2
PMA $10E^{-6}$	1.9 ± 0.7	293.0 ± 2.3	3.4 ± 0.3	0.9 ± 0.0	50.3 ± 1.5	1.5 ± 0.2	0.9 ± 0.1
PMA $10E^{-5}$	1.9 ± 0.1	299.5 ± 1.2	3.7 ± 0.2	0.9 ± 0.0	45.1 ± 2.2	1.5 ± 0.2	0.7 ± 0.0

Rs solution resistance, *Rm* resistance of the EPS film, *CPE_EPS* constant phase element of the EPS film, *CPE_dL* constant phase element of the interface, *Rct* ion transfer equivalent resistance, *µ* ion mobility

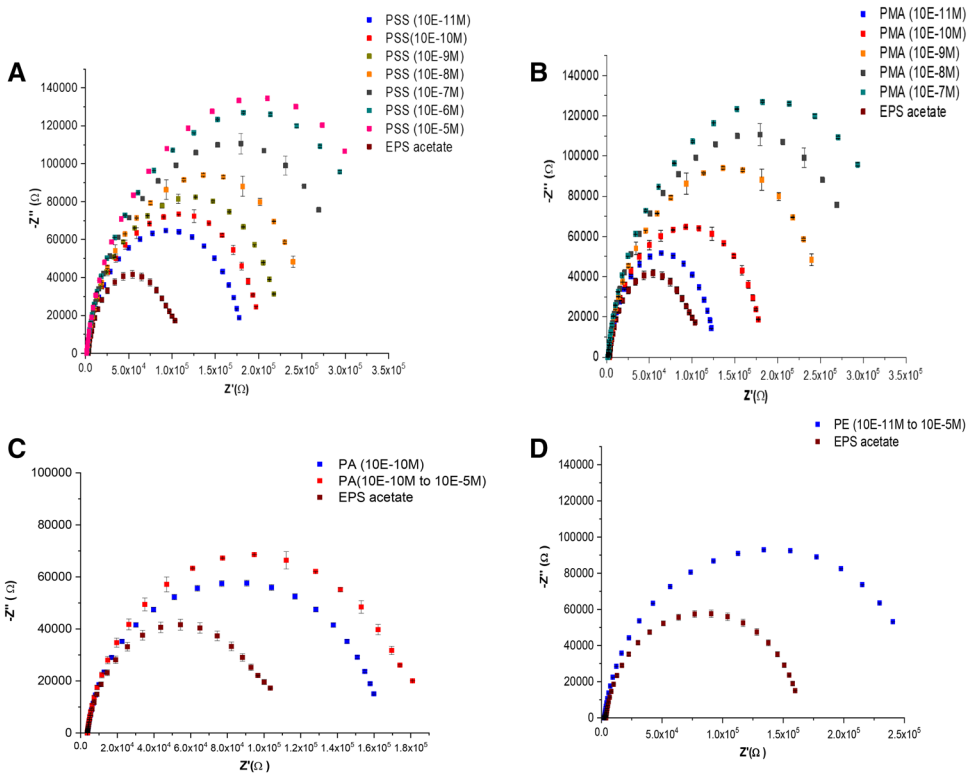

Fig.7 Nyquist diagram Z′ (real) vs Z″ (imaginary) of electrochemical impedance spectra for the microplastics detection [PSS (**A**), PMA (**B**), PA (**C**), and PE (**D**)] with the gold sensor coated with EPS film. Values are expressed as the mean six replicates (n = 6) ± standard deviation

EPS film (CPE_EPS) and the interface (CPE_dL). The ion transfers equivalent resistance (Rct) and the resistance of the solution (Rs), showed a decrease with the increase of the concentration. These results clearly signify that the microplastics solution were incrusted on the EPSs electrode which provide easier access for intercalation of ions on EPS electrode surface and easy charge-transfer at electrode–electrolyte interface [70].

The EPS resistance (Rm) increased with increasing the concentration of microplastics. Indeed, according to the pore-impedance relationship, the Rm can be attributed to the impediment to the microplastics passing through the pores. Several studies showed that small particles tend to aggregate into the pores in polymers and then adsorb to the surface wholly or individually [46].

Conclusion

This work demonstrates the validity of using EPS as a bioreceptor for the development of biosensors allowing the detection of low concentrations of different types of microplastics. The detection limits are 10^{-11} to 10^{-5} M, but the larger the particle size, the faster the saturation of the EPS membrane and the smaller the detection interval in terms of concentration. Investigations using the same type of biosensor for the detection of nanoparticles can be envisaged in this direction. However, more investigations are also needed to understand the behavior of the biosensor in the presence of a mixture of particles of different sizes.

EPS represent a natural substance, which is complex in its physical and chemical structure. The EPS film is monodisperse at the molecular scale with a homogeneous structure and adheres to the surface of the gold wafer without adding a specific ligand, which represents an advantage in the development of biosensors. However, its negative charge and the presence of different functional groups in its structure reduce its selectivity for plastic in a solution containing several types of pollutants. The use of the impedimetric biosensor thus designed in the field and the study of interactions with pollutants of different nature remains subject to additional investigations.

Supplementary Information The online version contains supplementary material available at https://doi.org/10.1007/s10924-022-02555-6.

Author Contributions All authors contributed to the conception of the manuscript and its drafting and approval.

Funding This research received no specific Grant from any funding agency in the public, commercial, or not-for-profit sectors.

Data Availability All data generated or analyzed during this study are included in the article.

Declarations

Conflict of interest The authors declare no conflict of interest.

Informed Consent No conflicts, informed consent, or human or animal rights apply to this study.

References

1. Kumar R et al (2021) Impacts of plastic pollution on ecosystem services, sustainable development goals, and need to focus on circular economy and policy interventions. Sustainability (Switzerland). https://doi.org/10.3390/su13179963
2. Galloway T, Haward M, Mason SA, Hardesty BD, Krause S (2020) Science-based solutions to plastic pollution. One Earth 2(1):5–7. https://doi.org/10.1016/j.oneear.2020.01.004
3. Lusher A, Hollman P, Mendoza-Hill J (2017) Microplastics in fisheries and aquaculture. Fisheries and Aquaculture Technical Paper. No. 615. Rome, Italy
4. Zbyszewski M, Corcoran PL (2011) Distribution and degradation of fresh water plastic particles along the beaches of Lake Huron, Canada. Water Air Soil Pollut 220(1–4):365–372. https://doi.org/10.1007/s11270-011-0760-6
5. Klein S, Worch E, Knepper TP (2015) Occurrence and spatial distribution of microplastics in river shore sediments of the rhine-main area in Germany. Environ Sci Technol 49(10):6070–6076. https://doi.org/10.1021/acs.est.5b00492
6. Tunali M, Uzoefuna EN, Tunali MM, Yenigun O (2020) Effect of microplastics and microplastic-metal combinations on growth and chlorophyll a concentration of *Chlorella vulgaris*. Sci Total Environ 743:140479. https://doi.org/10.1016/j.scitotenv.2020.140479
7. Rochman CM, Hoh E, Hentschel BT, Kaye S (2013) Classify plastic waste as hazardous (types of externalities caused by consumption of plastic bags). Environ Sci Technol 47(3):1646–1654
8. Rocha-Santos T, Duarte AC (2015) A critical overview of the analytical approaches to the occurrence, the fate and the behavior of microplastics in the environment. TrAC Trends Anal Chem 65:47–53. https://doi.org/10.1016/j.trac.2014.10.011
9. Shim WJ, Hong SH, Eo SE (2017) Identification methods in microplastic analysis: a review. Anal Methods 9(9):1384–1391. https://doi.org/10.1039/c6ay02558g
10. Zarfl C (2019) Promising techniques and open challenges for microplastic.pdf
11. Baruah A, Sharma A, Sharma S, Nagraik R (2022) An insight into different microplastic detection methods. Int J Environ Sci Technol 19(6):5721–5730. https://doi.org/10.1007/s13762-021-03384-1
12 Li J, Liu H, Paul Chen J (2018) Microplastics in freshwater systems: a review on occurrence, environmental effects, and methods for microplastics detection. Water Res 137:362–374. https://doi.org/10.1016/j.watres.2017.12.056
13. Maes T, Jessop R, Wellner N, Haupt K, Mayes AG (2017) A rapid-screening approach to detect and quantify microplastics based on fluorescent tagging with Nile Red. Sci Rep 7(February):1–10. https://doi.org/10.1038/srep44501
14. Silva AB, Bastos AS, Justino CIL, da Costa JP, Duarte AC, Rocha-Santos TAP (2018) Microplastics in the environment: challenges in analytical chemistry—a review. Anal Chim Acta 1017:1–19. https://doi.org/10.1016/j.aca.2018.02.043
15. Mai L, Bao LJ, Shi L, Wong CS, Zeng EY (2018) A review of methods for measuring microplastics in aquatic environments. Environ Sci Pollut Res 25(12):11319–11332. https://doi.org/10.1007/s11356-018-1692-0
16. Dümichen E, Eisentraut P, Bannick CG, Barthel AK, Senz R, Braun U (2017) Fast identification of microplastics in complex environmental samples by a thermal degradation method. Chemosphere 174:572–584. https://doi.org/10.1016/j.chemosphere.2017.02.010
17. Van Cauwenberghe L, Vanreusel A, Mees J, Janssen CR (2013) Microplastic pollution in deep-sea sediments. Environ Pollut 182:495–499. https://doi.org/10.1016/j.envpol.2013.08.013
18. Frias JPGL, Otero V, Sobral P (2014) Evidence of microplastics in samples of zooplankton from Portuguese coastal waters. Mar Environ Res 95:89–95. https://doi.org/10.1016/j.marenvres.2014.01.001
19. Löder MGJ, Kuczera M, Mintenig S, Lorenz C, Gerdts G (2015) Focal plane array detector-based micro-Fourier-transform infrared imaging for the analysis of microplastics in environmental samples. Environ Chem 12(5):563–581. https://doi.org/10.1071/EN14205
20. Mani T, Hauk A, Walter U, Burkhardt-Holm P (2015) Microplastics profile along the Rhine River. Sci Rep 5(December):1–7. https://doi.org/10.1038/srep17988
21. Mintenig SM, Int-Veen I, Löder MGJ, Primpke S, Gerdts G (2017) Identification of microplastic in effluents of waste water treatment plants using focal plane array-based micro-Fourier-transform infrared imaging. Water Res 108:365–372. https://doi.org/10.1016/j.watres.2016.11.015
22. Käppler A et al (2016) Analysis of environmental microplastics by vibrational microspectroscopy: FTIR, Raman or both? Anal Bioanal Chem 408(29):8377–8391. https://doi.org/10.1007/s00216-016-9956-3
23. McDermid KJ, McMullen TL (2004) Quantitative analysis of small-plastic debris on beaches in the Hawaiian archipelago. Mar Pollut Bull 48(7–8):790–794. https://doi.org/10.1016/j.marpolbul.2003.10.017
24. Quinn B, Murphy F, Ewins C (2017) Validation of density separation for the rapid recovery of microplastics from sediment. Anal Methods 9(9):1491–1498. https://doi.org/10.1039/c6ay02542k
25. Käppler A et al (2015) Identification of microplastics by FTIR and Raman microscopy: a novel silicon filter substrate opens the important spectral range below 1300 cm−1 for FTIR transmission measurements. Anal Bioanal Chem 407(22):6791–6801. https://doi.org/10.1007/s00216-015-8850-8
26. Lee J, Chae KJ (2021) A systematic protocol of microplastics analysis from their identification to quantification in water environment: a comprehensive review. J Hazard Mater 403:124049. https://doi.org/10.1016/j.jhazmat.2020.124049
27. Mazouz Z, Touchente ZA, Laradi H, Fourati N (2020) Design of novel electrochemical sensors for the selective detection of glyphosate. Multidiscip Digit Publish Inst Proc 1:2–5. https://doi.org/10.3390/proceedings1040483
28. Attoye B et al (2020) Developing a low-cost, simple-to-use electrochemical sensor for the detection of circulating tumour DNA in human fluids. Biosensors. https://doi.org/10.3390/bios10110156
29 Tamarin O, Rebi D, Dejous C (2020) Mobile acoustic wave platform deployment in the amazon river : impact of the water sample on the love wave sensor response. Sensors 20:72
30. Nagraik R, Kaushal A, Gupta S, Sethi S, Sharma A, Kumar D (2020) Nanofabricated versatile electrochemical sensor for *Leptospira interrogans* detection. J Biosci Bioeng 129(4):441–446. https://doi.org/10.1016/j.jbiosc.2019.11.003
31. Asamoah BO, Kanyathare B, Roussey M, Peiponen KE (2019) A prototype of a portable optical sensor for the detection of transparent and translucent microplastics in freshwater. Chemosphere 231:161–167. https://doi.org/10.1016/j.chemosphere.2019.05.114
32. Malyuskin O (2020) Microplastic detection in soil and water using resonance microwave spectroscopy: a feasibility study. IEEE Sens J 20(24):14817–14826. https://doi.org/10.1109/JSEN.2020.3011311
33 Tekaya N et al (2013) Acoustic, electrochemical and microscopic characterization of interaction of *Arthrospira platensis* biofilm and

heavy metal ions. J Environ Chem Eng. https://doi.org/10.1016/j.jece.2013.07.006
34. Naresh V, Lee N (2021) A review on biosensors and recent development of nanostructured materials-enabled biosensors. Sensors (Switzerland) 21(4):1–35. https://doi.org/10.3390/s21041109
35. Bhalla N, Jolly P, Formisano N, Estrela P (2016) Introduction to biosensors. Essays Biochem 60(1):1–8. https://doi.org/10.1042/EBC20150001
36. Mehrotra P (2016) Biosensors and their applications—a review. J Oral Biol Craniofacial Res 6(2):153–159. https://doi.org/10.1016/j.jobcr.2015.12.002
37. Woo H et al (2022) Sensitive and specific capture of polystyrene and polypropylene microplastics using engineered peptide biosensors. RSC Adv 12(13):7680–7688. https://doi.org/10.1039/d1ra08701k
38 Baracu AM, DinuGugoasa LA (2021) Review—recent advances in microfabrication, design and applications of amperometric sensors and biosensors. J Electrochem Soc 168(3):037503. https://doi.org/10.1149/1945-7111/abe8b6
39 Huang CJ, Narasimha GV, Chen YC, Chen JK, Dong GC (2021) Measurement of low concentration of micro-plastics by detection of bioaffinity-induced particle retention using surface plasmon resonance biosensors. Biosensors. https://doi.org/10.3390/bios11070219
40 Xiao R, Zheng Y (2016) Overview of microalgal extracellular polymeric substances (EPS) and their applications. Biotechnol Adv 34(7):1225–1244. https://doi.org/10.1016/j.biotechadv.2016.08.004
41 Delattre C, Pierre G, Laroche C, Michaud P (2016) Production, extraction and characterization of microalgal and cyanobacterial exopolysaccharides. Biotechnol Adv 34(7):1159–1179. https://doi.org/10.1016/j.biotechadv.2016.08.001
42. Gongi W, Pinchetti JLG, Cordeiro N, Sadok S, Ben Ouada H (2021) Characterization of biodegradable films based on extracellular polymeric substances extracted from the thermophilic microalga *Graesiella* sp. Algal Res. https://doi.org/10.1016/j.algal.2021.102565
43. Saravanan C, Kavitake D, Kandasamy S, Devi PB, Shetty PH (2019) Production, partial characterization and antioxidant properties of exopolysaccharide α-d-glucan produced by Leuconostoc lactis KC117496 isolated from an idli batter. J Food Sci Technol 56(1):159–166. https://doi.org/10.1007/s13197-018-3469-3
44. Zhu C et al (2012) Bioflocculant produced by *Chlamydomonas reinhardtii*. J Appl Phycol 24(5):1245–1251. https://doi.org/10.1007/s10811-011-9769-x
45. Wang L, Auty MAE, Kerry JP (2010) Physical assessment of composite biodegradable films manufactured using whey protein isolate, gelatin and sodium alginate. J Food Eng 96(2):199–207. https://doi.org/10.1016/j.jfoodeng.2009.07.025
46. Lagarde F, Olivier O, Zanella M, Daniel P, Hiard S, Caruso A (2016) Microplastic interactions with freshwater microalgae: hetero-aggregation and changes in plastic density appear strongly dependent on polymer type. Environ Pollut 215:331–339. https://doi.org/10.1016/j.envpol.2016.05.006
47. Zamfir LG, Puiu M, Bala C (2020) Advances in electrochemical impedance spectroscopy detection of endocrine disruptors. Sensors (Switzerland) 20(22):1–21. https://doi.org/10.3390/s20226443
48. Gongi W, Cordeiro N, Pinchetti JLG, Sadok S, Ben Ouada H (2021) Extracellular polymeric substances with high radical scavenging ability produced in outdoor cultivation of the thermotolerant chlorophyte *Graesiella* sp. J Appl Phycol 33(1):357–369. https://doi.org/10.1007/s10811-020-02303-0
49. Mezhoud N, Zili F, Bouzidi N, Helaoui F, Ammar J, Ben Ouada H (2014) The effects of temperature and light intensity on growth, reproduction and EPS synthesis of a thermophilic strain related to the genus *Graesiella*. Bioprocess Biosyst Eng 37(11):2271–2280. https://doi.org/10.1007/s00449-014-1204-7
50. Dubois M, Gilles K, Hamilton J, Rebers P, Smith F (1965) Colorimetric method for the determination of sugars and related substances – ScienceOpen. Available from: https://www.scienceopen.com/document?vid=8f3823b9-b461-49b4-8e91-a93572357775. Accessed 17 Mar 2021
51. Lowry OH, Roserbough NJ, Farr AL, Randall RJ (1951) Protein measurement with the Folin phenol reagent. J Biol Chem 193(1):265–275. https://doi.org/10.1016/s0021-9258(19)52451-6
52. Mishra A, Kavita K, Jha B (2011) Characterization of extracellular polymeric substances produced by micro-algae *Dunaliella salina*. Carbohydr Polym 83(2):852–857. https://doi.org/10.1016/j.carbpol.2010.08.067
53. Delgado AV, González-Caballero F, Hunter RJ, Koopal LK, Lyklema J (2005) Measurement and interpretation of electrokinetic phenomena: (IUPAC technical report). Pure Appl Chem 77(10):1753–1805. https://doi.org/10.1351/pac200577101753
54. Touzi H, Chevalier Y, Martin M, Ben Ouada H, Jaffrezic-Renault N (2021) Detection of gadolinium with an impedimetric platform based on gold electrodes functionalized by 2-methylpyridine- substituted cyclam. Sensors 21(5):1658
55 De Philippis R, Sili C, Paperi R, Vincenzini M (2001) Exopolysaccharide-producing cyanobacteria and their possible exploitation: a review. J Appl Phycol. https://doi.org/10.1023/A:1017590425924
56. Miao T, Wang J, Zeng Y, Liu G, Chen X (2018) Polysaccharide-based controlled release systems for therapeutics delivery and tissue engineering: from bench to bedside. Adv Sci. https://doi.org/10.1002/advs.201700513
57. Parwani L, Bhatnagar M, Bhatnagar A, Sharma V (2014) Antioxidant and iron-chelating activities of cyanobacterial exopolymers with potential for wound healing. J Appl Phycol 26(3):1473–1482. https://doi.org/10.1007/s10811-013-0180-7
58. Danaei M et al (2018) Impact of particle size and polydispersity index on the clinical applications of lipidic nanocarrier systems. Pharmaceutics 10(2):1–17. https://doi.org/10.3390/pharmaceutics10020057
59. Santhiya D, Subramanian S, Natarajan KA (2002) Surface chemical studies on sphalerite and galena using extracellular polysaccharides isolated from *Bacillus polymyxa*. J Colloid Interface Sci 256(2):237–248. https://doi.org/10.1006/jcis.2002.8681
60. Jridi M et al (2014) Physical, structural, antioxidant and antimicrobial properties of gelatin-chitosan composite edible films. Int J Biol Macromol 67:373–379. https://doi.org/10.1016/j.ijbiomac.2014.03.054
61. Li WW, Zhou WZ, Zhang YZ, Wang J, Zhu XB (2008) Flocculation behavior and mechanism of an exopolysaccharide from the deep-sea psychrophilic bacterium *Pseudoalteromonas* sp. SM9913. Bioresour Technol 99(15):6893–6899. https://doi.org/10.1016/j.biortech.2008.01.050
62 De Jesus Raposo MF, De Morais RMSC, De Morais AMMB (2013) Bioactivity and applications of sulphated polysaccharides from marine microalgae. Mar Drugs 11(1):233–252. https://doi.org/10.3390/md11010233
63. Cunha C, Faria M, Nogueira N, Ferreira A, Cordeiro N (2019) Marine vs freshwater microalgae exopolymers as biosolutions to microplastics pollution. Environ Pollut 249:372–380. https://doi.org/10.1016/j.envpol.2019.03.046
64. Restrepo-Flórez JM, Bassi A, Thompson MR (2014) Microbial degradation and deterioration of polyethylene—a review. Int Biodeterior Biodegrad 88:83–90. https://doi.org/10.1016/j.ibiod.2013.12.014
65. Mota R et al (2015) Effects of heavy metals on *Cyanothece* sp. CCY 0110 growth, extracellular polymeric substances (EPS)

production, ultrastructure and protein profiles. J Proteomics 120:75–94. https://doi.org/10.1016/j.jprot.2015.03.004
66. Xu Y, Xie X, Duan Y, Wang L, Cheng Z, Cheng J (2016) A review of impedance measurements of whole cells. Biosens Bioelectron 77:824–836. https://doi.org/10.1016/j.bios.2015.10.027
67 Macdonald K (1992) Warmth as a developmental construct : an evolutionary analysis. Child Dev 63(4):753–773
68 Zhu X, Zhao W, Chen X, Zhao T, Tan L, Wang J (2020) Growth inhibition of the microalgae *Skeletonema costatum* under copper nanoparticles with microplastic exposure. Mar Environ Res 158(May):105005. https://doi.org/10.1016/j.marenvres.2020.105005
69 Chae Y, Kim D, An YJ (2019) Effects of micro-sized polyethylene spheres on the marine microalga *Dunaliella salina*: focusing on the algal cell to plastic particle size ratio. Aquat Toxicol 216(September):105296. https://doi.org/10.1016/j.aquatox.2019.105296
70. Uke SJ, Mardikar SP, Bambole DR, Kumar Y, Chaudhari GN (2020) Sol-gel citrate synthesized Zn doped MgFe2O4 nanocrystals: a promising supercapacitor electrode material. Mater Sci Energy Technol 3:446–455. https://doi.org/10.1016/j.mset.2020.02.009